Metrics Analysis Framework of Control and Management System for Resilient Connected Community Microgrids

Behnaz Papari, *Member, IEEE*, Christopher S. Edrington, *Senior Member, IEEE*, Mojtaba Ghadamyari, *Member, IEEE*, Mostafa Ansari, *Member, IEEE*, Gokhan Ozkan, *Member, IEEE*, and Badrul Chowdhury, *Senior Member, IEEE*

***Abstract*—This paper proposes a novel metrics analysis of the control and management system for an efficient and resilient post-hurricane integrated recovery framework. To enhance the resiliency of networked-microgrids (MGs), resources such as mobile emergency resources (MERs), electric vehicles (EVs), and energy storage systems (ESSs) associated with the reconfiguration strategy are utilized to decrease blackouts to a minimum time. In the proposed method, the local power-flow path is actively altered by the network reconfiguration. This capability allows restoring critical loads and minimizing the energy not supplied (ENS) to the local consumers. Islanded loads that need truck-mounted MERs are simultaneously determined through optimal scheduling. The role of MERs is to deliver power to the islanded load regarding optimal routes. To produce optimal routes and to avoid out-of-service roads, the well-known Dijkstra's algorithm is used in this study. The proposed method aims to maximize system resiliency through the integrated single-objective optimization problem, associated with evaluating the metrics, to assess the control system performance from a resiliency index perspective. Simulation results on a 69-bus test system indicate satisfactory performance and effectiveness of the proposed method.**

***Index Terms*—Integrated resilient framework, mobile emergency resources, networked microgrids, electrical vehicle, energy storage systems, metrics assessment.**

Manuscript received January 12, 2021; revised May 10, 2021 and September 23, 2021; accepted November 2, 2021. Date of publication November 19, 2021; date of current version March 22, 2022. This work was supported by the Department of Energy under Grant DE-EE0008607. Paper no. TSTE-00049-2021. *(Corresponding author: Behnaz Papari.)*

Behnaz Papari is with Automotive Engineering and Electrical and Computer Engineering Departments, Clemson University, Clemson, SC 29634 USA (e-mail: bpapari@uncc.edu).

Christopher S. Edrington is with the Holcombe Department of Electrical and Computer Engineering, Clemson University, Clemson, SC 29634 USA (e-mail: cedring@clemson.edu).

Mojtaba Ghadamyari is with the Department of Electrical Engi neering, Shahid Beheshti University, Tehran 1983963113, Iran (e-mail: ghadamyari.moj@gmail.com).

Mostafa Ansari is with the Isfahan University of Technology, Isfahan 8415683111, Iran (e-mail: ansari.mostafa70@gmail.com).

Gokhan Ozkan is with Electrical and Computer Engineering, Clemson University, Clemson, SC 29634 USA (e-mail: gokhano@clemson.edu).

Badrul Chowdhury is with Electrical and Computer Engineering, University of North Carolina at Charlotte, Charlotte, NC 28223 USA (e-mail: b.chowdhury@uncc.edu).

Color versions of one or more figures in this article are available at https://doi.org/10.1109/TSTE.2021.3129450.

Digital Object Identifier 10.1109/TSTE.2021.3129450

NOMENCLATURE

A. Sets/Indices

t, s	Index of time periods and scenario
g, k, e, i, m	Index of DG unit, MG, ESS, PV unit, MERs
j, h	Index of EV's stations and number of EVs
b, b'	indices of buses with DG units
l, d	index of distribution lines and load demand

B. Constants

$\underline{C_m^S}, \overline{C_m^S}$	Minimum/maximum allowable stored energy (kWh)
CT_m^S, DT_m^S	Minimum charging/discharging time (hr)
$\overline{I^L}$	Maximum current flow of distribution lines (A)
$\underline{P_{g,k}^{DG}}, \overline{P_{g,k}^{DG}}$	Minimum/maximum active power of DG units (kW)
$\underline{P_{m,k}^{MER}}, \overline{P_{m,k}^{MER}}$	Minimum/maximum active power of MERs (kW)
$\underline{Q_{g,k}^{DG}}, \overline{Q_{g,k}^{DG}}$	Minimum/maximum reactive power of DG units (kVar)
$\underline{Q_{m,k}^{MER}}, \overline{Q_{m,k}^{MER}}$	Minimum/maximum reactive power of MERs (kVar)
$\underline{P_{j,h,k}^{EV,Ch}}, \overline{P_{j,h,k}^{EV,Ch}}$	Minimum/maximum charging power of EV (kW)
$\underline{P_{j,h,k}^{EV,Dch}}, \overline{P_{j,h,k}^{EV,Dch}}$	Minimum/maximum discharging power of EV (kW)
$\underline{P_{k,e}^{ESS,Ch}}, \overline{P_{k,e}^{ESS,Ch}}$	Minimum/maximum charging power of ESS (kW)
$\underline{P_{t,d,k}^{DR}}, \overline{P_{t,d,k}^{DR}}$	Active power limitations in DR program
$\underline{Q_{t,d,k}^{DR}}, \overline{Q_{t,d,k}^{DR}}$	Reactive power limitations in DR program
$\underline{P_{k,e}^{ESS,Dch}}, \overline{P_{k,e}^{ESS,Dch}}$	Minimum/maximum discharging power of ESS (kW)
$\underline{SOC_{m,k}^{MER}}$	Lower boundary of MERs SOC (%)

$\overline{SOC^{ESS}_{k,e}}, \underline{SOC^{ESS}_{k,e}}$ Upper/lower boundary of MERs SOC (%)

$\overline{SOC^{EV}_{k,j,h}}, \underline{SOC^{EV}_{k,j,h}}$ Upper/lower boundary of EV SOC (%)

$Cap^{ESS}_{k,e}$ Battery capacity (kW)

r, x, δ Resistance/reactance of distribution lines (ohm)

Z^{LQ}, Z^{LP} Slack variables to make the power equality constraints valid

F^A, F^B Indicating electrical characteristic of the lines

$RU^{DG}_{g,k}, RD^{DG}_{g,k}$ Ramp up/down rate of DG units (kW)

T^O, T_{CL} Restoration time-period and service time of the load in post-hurricane restoration (hr)

UT^G_m, DT^G_m Minimum up/down time of DG units (kW)

$\underline{V}, \overline{V}$ Minimum/maximum voltage magnitude limits (V)

$\pi^{DG}_{g,k}$ Generation cost ($/kW)

$W_{m,k}$ Weight (significance) of the load on *m*th bus

β_i Weight factors in operation cost function

$\eta^{Ch}_m, \eta^{Disch}_m$ Charging/discharging efficiency

$G^{STC}, P^{STC}_{k,i}, G^{INC}_{s,t,k,i}$ Parameters of PVs' power generation

t_r Hurricane time (hr)

T_c, T_r Ambient and reference temperature (F)

$T^{Ch}_{m,k,t}, T^{Disch}_{m,k,t}$ Number of successive charging/ discharging hours (hr)

$T^{DG-on}_{s,g,k,t}, T^{DG-off}_{s,g,k,t}$ Number of successive on/off hours for DGs (hr)

C. Variables

$P^D_{s,t,d,k}, Q^D_{s,t,d,k}$ Scheduled active/reactive power demand (kW/kVar)

$P^{D_0}_{t,d,k}, Q^{D_0}_{t,d,k}$ Initial scheduled active/reactive power demand (kW/kVar)

$\Delta P^D_{s,t,d,k}, \Delta Q^D_{s,t,d,k}$ Change in price/demand

$P^{Demand}_{s,t,d,k}, Q^{Demand}_{s,t,d,k}$ Real active/reactive power demand (kW/kVar)

$P^{DR}_{s,t,d,k}, Q^{DR}_{s,t,d,k}$ Reactive/active power in DR program

$P^{shed}_{s,t,d,k}, Q^{shed}_{s,t,d,k}$ Load shedding (kW/kVar)

$P^{EV}_{s,t,k,j,h}, P^{TEV}_{s,t,k,j}$ Injection power of EVs (kW)

$P^{PV}_{s,t,k,i}, Q^{PV}_{s,t,k,i}$ Output power of PV unit (kWh)

$P^L_{mn,k,t}, Q^L_{mn,k,t}$ Active/reactive power flow of distribution lines (kW/kVar)

$P^{DG}_{s,g,k,t}, Q^{DG}_{s,g,k,t}$ Active/reactive power of DG units (kW/kVar)

$P^{MER}_{m,k}, Q^{MER}_{m,k}$ Active/reactive power of MERs (kW/kVar)

$V_{s,t,k,b(b')}$ Buss voltage

$x^{DG}_{s,g,k,t}, x^{MER}_{s,m,k,t}$ Binary variable for the state of DG and MERs

$t^{AR}_{k,j,h,s}, t^{DP}_{k,j,h,s}$ Binary variable for arriving and departure time of EVs

I. Introduction

EXTREME weather events, known as low-probability, high-impact (LPHI) events, have caused severe problems in power grids, resulting in economic losses, power quality deterioration, and more importantly, long-term load outages [1]. Seven major storms have led to over one billion dollars each in heavy damages during the last ten years. In the US, more than 80% of blackouts, which involved over 50000 people per blackout, are mainly caused by hurricanes and major storms [2]. When hurricane Harvey struck in August 2017, it generated 180 billion dollars in damages to infrastructure. Consequently, a long-term blackout occurred, which lasted over a few weeks in the connected community. Some of the other weather-related events in recent years, such as the 2019 hurricane Dorian, 2018 hurricane Michael, 2017 hurricane Maria, and 2016 hurricane Matthew which struck the US and other countries resulted in damages to power system infrastructures and so led to long-term blackouts [3], [4].

Weather-related disasters, such as those aforementioned, have posed several issues regarding resiliency of electrical systems. Respectively, resilience is defined as the capability of an electrical grid to withstand, adapt and recover from extreme disturbances. According to this definition, resilient systems are those that maintain a proactive consciousness of surrounding threats and adequately react to return the system to normal operating conditions in a finite time [5].

Several scientific studies have been performed to investigate the resilience of electrical systems and a couple of models based on resilience and reinforcement schemes have been proposed [6]–[8]. Microgrids (MGs) are typically proposed to be utilized as critical resources to improve the power system's resilience during extreme events [9]. To restore the electrical loads, MGs accompanied by DGs are used in [10]. In [11], MGs are leveraged to evaluate the availability of electrical load restoration and time of service by defining the concept of continuous operating time. The idea of MG is used to alleviate the congestion level of feeders in the outage area in [12]. Authors of [13], proposed an efficient strategy for MGs' resilience enhancement which reduces restoration time after the disruptive event occurrence. Researchers in [14] developed an operational distribution algorithm for post-disaster restoration of critical loads using multiple MGs formations. Self-healing capabilities of resilient MGs are reviewed in [15]. The authors of [16] presented a self-healing strategy for optimal scheduling of DGs in faulty and normal conditions. In [17], authors concluded that resilient power grids by incorporating MGs in distribution systems.

The reviewed research studies primarily concentrated on electrical grids and neglected damages regarding other critical infrastructure. Technically, connected community microgrids (CCMGs) are an essential grid infrastructure that provides more reliable electricity to customers. However, geographical failures caused by lack of vegetation management on critical

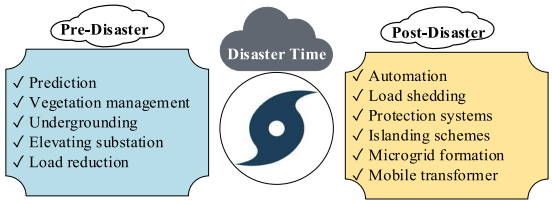

Fig. 1. Strategies for electric grid usage after and before a natural disaster.

infrastructures such as roads, bridges, and streets, will reduce this superiority over the typical types of the grid structures. Thus, finding an appropriate approach to relieve the effects of natural disasters, by providing an optimum solution to supply electricity for the customers, effectively increases the networks' reliability and resiliency. Therefore, there is an essential need for a practical resilient framework, which maximizes operational capacity by addressing damages on other infrastructures. Moreover, the authors of [18] assessed the interdependency of critical infrastructures in electrical load restoration after the weather event. It was revealed that physical constraints need to be considered as part of the feasible operation of power system because of such extreme circumstances.

As observed from the literature review, weather-related disasters such as hurricanes have led to significant research studies mainly due to the high complexity and unpredictability of such events. Resilience enhancement methods are usually divided into three main groups based on the response timeline of the electrical grid in the case of a hurricane. In the pre-hurricane phase, the power equipment outage is predicted, and the electrical grid is prepared for any upcoming event through vegetation, hardening, etc. [10]. During the hurricane, some actions are appropriately taken, namely network reconfiguration, backup generators, and rescheduling of available resources [19]. In the post-hurricane phase, by reconfiguring the network and re-energizing the power network (usually black-start generation), the network is returned back to the normal operating conditions [20]. Some other available strategies for improving system resilience are listed in Fig. 1.

Many of the recent works that performed post-hurricane analyses mainly concentrated on re-energizing electrical loads using DGs and MGs. Reference [21] investigates the optimal switching as a fast and practical load restoration tool. In [22], the authors performed a comprehensive assessment of the role of DGs and switches in restoring electrical loads using automation technology. Despite the effectiveness of previous methods in recent studies, very few of them considered mobile emergency resources (MERs), and none of them thought the metrics assessment in the rapid recovery of electrical loads.

In [23]–[25], a two-stage post-hurricane recovery model is proposed to maximize the resilience of networked MGs. In pre-positioning, MERs are located at suitable locations, while in real-time allocation, which occurs after a natural disaster, MERs are dispatched as DGs to restore electrical loads. However, they neglected to consider the interdependency of the critical transportation infrastructure in restored loads. In [26], a two-stage framework was proposed to restore the electrical loads based on mixed-integer non-linear programming (MINLP).

TABLE I
SCOPES SUMMARY OF THE PREVIOUS STUDIES

Ref	Scope					
	MG	CCMG	Practicality	Metric Assessment	Real-time	Accuracy
[6-9]	✓	×	×	×	×	×
[10-14]	✓	×	×	×	×	✓
[15-17]	✓	×	×	×	×	✓
[18-20]	✓	×	✓	×	×	✓
[21-22]	✓	×	✓	×	×	×
[23,24]	×	✓	✓	✓	×	✓
[25]	×	✓	✓	×	✓	✓
[26]	✓	×	✓	×	×	✓
[27]	×	✓	✓	×	×	✓
[28]	×	✓	✓	×	✓	✓
[29]	×	✓	×	✓	✓	×
[30]	×	✓	×	×	×	✓

It is clear from the literature review, the resiliency assessment of the power networks is a complex problem correlated with several critical infrastructure sectors such as social/cultural, economic, lifestyle, environmental, security, public health, and safety. Thus, various approaches are proposed in the literature to improve the resiliency index w.r.t. each specific critical infrastructure sector. In addition, each sector is integrated with other sub-sectors, which require proper determination for enhancing the resiliency of the power networks in order to rebound after weather-related disasters [27]. The latest research efforts [28]–[30] are compared with this study based on their scope, and motivation in Table I for better visualization.

The main contributions of this study are summarized in the bullet points below:

- The resilience enhancement of CCMGs based on MERs, EVs, DGs, and controlled switches
- The control and management system assessment by quantifiable and verifiable metrics analysis is considered to fulfill the performance-based rate (PBR) requirements
- The detailed formulation of transportation sector (8)–(10) such as MERs cooperation on grid restoration
- Developing an appropriate approach with the potential for real-time instantiation
- Developing the metrics assessment of the control framework based on voltage deviation, performance, loss, and restored loads
- Reconfiguration of distribution networks relies upon the MERs availability and controlled switches

The concept of cooperative power scheduling commitment can help enhance the resilience of networked MGs in emergencies. Therefore, a novel integrated management and operation framework is proposed to strengthen the networked MGs by optimizing both restoration time, and the amount of restored critical loads. Thus, simultaneous scheduling, and operation of MGs resources and MERs short-path routing are effectively conducted by a reconfiguration scheme to change the topology of networked MGs and supply substitute paths for electrifying the interrupted loads. Truck-mounted MERs are simultaneously deployed to deliver power to the islanded buses and the ones with loss/shortages of power based on the limitations of the post-hurricane transportation infrastructure and possible shortest path target. The DR (demand response) program is also deployed in this study to control some of the loads.

The rest of this paper is organized as follows. Section II explains the problem formulation, component modeling and elaborates on the objective and relevant constraints. Section III describes Dijkstra's algorithm as the shortest path exploration algorithm. Section IV presents illustrative scenarios and simulation results of the proposed model applied to a networked MGs test system. Discussion on the metrics assessment of the proposed control system is provided in Sections V. Section VI concludes the study by summarizing key contributions and potential practical applications.

II. Problem Formulation and Component Modeling

In this section, problem formulation, including operational constraints and objective function, is developed. Furthermore, the electrical components and MG distribution network are modeled. The implemented formulation and models are used in the suggested resilient optimization problem.

A. Load Constraints and DR Program

It is assumed that the distribution network operator (DNO) can directly manage some of the electric loads by utilizing photovoltaic (PV) units, remote control switches, and the DR program. In (1), the value of active and reactive supplied power is shown. According to (1), applying the load control to the active power would reduce the reactive power of the same load.

$$\begin{cases} P^{D}_{s,t,d,k} = P^{D_0}_{t,d,k} + \Delta P^{D}_{s,t,d,k} \\ Q^{D}_{s,t,d,k} = Q^{D_0}_{t,d,k} + \Delta Q^{D}_{s,t,d,k} = P^{D}_{s,t,d,k} \times \tan\varphi_{t,d,k} \end{cases} \tag{1}$$

The DNO utilizing the DR program controls the loads on the demand-side; which results in the optimal and resilient operation of the system after the occurrence of the hurricane. Constraints (2)–(3) show the difference in the scheduled and deployed amount of the DR program.

$$\begin{cases} P^{Demand}_{s,t,d,k} = P^{D}_{s,t,d,k} - P^{DR}_{s,t,d,k} \\ P^{DR}_{s,t,d,k} \le \overline{P^{DR}_{t,d,k}} \end{cases} \tag{2}$$

$$\begin{cases} Q^{Demand}_{s,t,d,k} = Q^{D}_{s,t,d,k} - Q^{DR}_{s,t,d,k} \\ Q^{DR}_{s,t,d,k} \le \overline{Q^{DR}_{t,d,k}} \end{cases} \tag{3}$$

Operational constraints, as formulated in (4)–(5), indicate the active and reactive power limits of a DG, (6) represents the limitations of ramp-up and ramp-down rates, and (7) shows the minimum up/down time limitations.

$$\begin{cases} \underline{P^{DG}_{g,k}} x^{DG}_{s,g,k,t} \le P^{DG}_{s,g,k,t} \le \overline{P^{DG}_{g,k}} x^{DG}_{s,g,k,t} \\ \underline{Q^{DG}_{g,k}} x^{DG}_{s,g,k,t} \le Q^{DG}_{s,g,k,t} \le \overline{Q^{DG}_{g,k}} x^{DG}_{s,g,k,t} \end{cases} \tag{4}$$

$$\begin{cases} P^{DG}_{s,g,k,t} = P^{DG_0}_{s,g,k,t-1} + \Delta P^{DG}_{s,g,k,t} \\ Q^{DG}_{s,g,k,t} = Q^{DG_0}_{s,g,k,t-1} + \Delta Q^{DG}_{s,g,k,t} \end{cases} \tag{5}$$

$$\begin{cases} P^{DG}_{s,g,k,t} - P^{DG}_{s,g,k,t-1} \le RU^{DG}_{g,k} \\ P^{DG}_{s,g,k,t-1} - P^{DG}_{s,g,k,t} \le RD^{DG}_{g,k} \end{cases} \tag{6}$$

$$\begin{cases} T^{DG-on}_{s,g,k,t} \ge UT^{DG}_{g,k} \left(x^{DG}_{s,g,k,t} - x^{DG}_{s,g,k,t-1} \right) \\ T^{DG-off}_{s,g,k,t} \ge DT^{DG}_{g,k} \left(x^{DG}_{m,k,t-1} - x^{DG}_{s,g,k,t} \right) \end{cases} \tag{7}$$

B. Truck-mounted MERs Constraints

The novel physical modeling of truck-mounted MERs is formulated. Limits (8)–(12) represent the proposed model for MERs operation in the network. Through (8) and (9), the active and reactive power capacity limitations of MERs and their status are ensured, respectively. The MERs state of charge (SOC) is calculated by (11) according to the available active power of MERs. In (12), the lower boundary of MERs SOC is considered.

$$\begin{cases} \underline{P^{MER}_{m,k}} x^{MER}_{s,m,k,t} \le P^{MER}_{s,m,k,t} \le \overline{P^{MER}_{m,k}} x^{MER}_{s,m,k,t} \\ \underline{Q^{MER}_{m,k}} x^{MER}_{s,m,k,t} \le Q^{MER}_{s,m,k,t} \le \overline{Q^{MER}_{m,k}} x^{MER}_{s,m,k,t} \end{cases} \tag{8}$$

$$\sum_{m} x^{MER}_{s,m,k,t} \le \overline{x^{MER}_{s,k,t}} \tag{9}$$

$$DT^{MER}_{m,k} \left(x^{MER}_{s,m,k,t} - x^{MER}_{s,m,k,t-1} \right) \le T^{MER}_{s,m,k,t} \tag{10}$$

$$SOC^{MER}_{s,m,k,t} = SOC^{MER}_{s,m,k,t-1} - \eta^{MER}_{m,k} \times P^{MER}_{s,m,k,t} \tag{11}$$

$$SOC^{MER}_{s,m,k,t} \ge \underline{SOC^{MER}_{m,k}} \tag{12}$$

C. Energy Storage Systems Constraints

Energy storage systems (ESSs) are practical resilience resources, which frequently have been used in recent studies. This study also utilizes ESSs in the proposed framework based on the utilized model in [31]. Constraint (13) calculates ESS SOC in different time intervals, (14) represents the charging and discharging limitations of the ESS, (15) shows the maximum and minimum level of SOC, and (16) represents binary variables indicating charging and discharging of ESSs.

$$SOC^{ESS}_{s,m,k,t} = SOC^{ESS}_{s,m,k,t-1} + \left(\eta^{ESS,Ch}_{k,e} \times P^{ESS,Ch}_{s,m,k,t} - P^{ESS,Ch}_{s,m,k,t} \Big/ \eta^{ESS,Dch}_{k,e} \right) \Big/ Cap^{ESS}_{k,e} \tag{13}$$

$$\begin{cases} x^{ESS,Ch}_{s,e,k,t} \times \underline{P^{ESS,Ch}_{k,e}} \le P^{ESS,Ch}_{s,e,k,t} \\ \le x^{ESS,Ch}_{s,e,k,t} \times \overline{P^{ESS,Ch}_{k,e}} \\ x^{ESS,Dch}_{s,e,k,t} \times \underline{P^{ESS,Dch}_{k,e}} \le P^{ESS,Dch}_{s,e,k,t} \\ \le x^{ESS,Dch}_{s,e,k,t} \times \overline{P^{ESS,Dch}_{k,e}} \end{cases} \tag{14}$$

$$\underline{SOC^{ESS}_{k,e}} \le SOC^{ESS}_{s,t,k,e} \le \overline{SOC^{ESS}_{k,e}} \tag{15}$$

$$x^{ESS,Ch}_{s,e,k,t} + x^{ESS,Dch}_{s,e,k,t} \le 1 \tag{16}$$

D. Electric Vehicles (EVs) Constraints

EVs are emerging resources of the resilience MGs. In this study, EVs and charging/discharging stations which are located at busses 4, 17, and 68 and are modeled in the proposed framework. Constraint (17) computes the output power of EVs based on the charging and discharging power, (18) shows the charging and discharging limits of the EVs, (19) indicates SOC of EVs'

batteries in different time intervals, (20) presents the maximum and minimum SOC level of EVs' batteries, (21) states that SOC level of EVs' batteries at arriving time equals to the initial SOC level of EVs' batteries, (22) represents binary variables indicating charging and discharging of EVs, (23) also shows binary variables indicating arriving/departure of EVs to/from the stations.

$$P^{EV}_{s,k,t,j,h} = P^{EV,Dch}_{s,k,t,j,h} - P^{EV,Ch}_{s,k,t,j,h} \tag{17}$$

$$\begin{cases} x^{EV,Ch}_{s,t,k,j,h} \times \underline{P^{EV,Ch}_{j,h,k}} \le P^{EV,Ch}_{s,t,k,j,h} \le x^{EV,Ch}_{s,t,k,j,h} \times \overline{P^{EV,Ch}_{j,h,k}} \\ x^{EV,Dch}_{s,t,k,j,h} \times \underline{P^{EV,Dch}_{j,h,k}} \le P^{EV,Dch}_{s,t,k,j,h} \le x^{EV,Dch}_{s,t,k,j,h} \times \overline{P^{EV,Dch}_{j,h,k}} \end{cases} \tag{18}$$

$$SOC^{EV}_{s,t,k,j,h} = SOC^{EV}_{s,t-1,k,j,h} + \left(\eta^{EV,Ch}_{k,j,h} \times P^{EV,Ch}_{s,t,k,j,h} - P^{EV,DCh}_{s,t,k,j,h} \Big/ \eta^{EV,Dch}_{k,j,h}\right) \Big/ Cap^{ESS}_{k,j,h} \tag{19}$$

$$\underline{SOC^{EV}_{k,j,h}} \le SOC^{EV}_{s,t,k,j,h} \le \overline{SOC^{EV}_{k,j,h}} \tag{20}$$

$$SOC^{EV}_{k,j,h,(t=t^{AR}_{kjhs})} = SOC^{EV}_{k,j,h,0} \tag{21}$$

$$x^{EV,Ch}_{s,t,k,j,h} + x^{EV,Dch}_{s,t,k,j,h} \le 1 \tag{22}$$

$$t^{AR}_{k,j,h,s} + t^{DP}_{k,j,h,s} \le 1 \tag{23}$$

$$P^{TEV}_{s,t,k,j} = \sum_{h} P^{EV}_{s,t,k,j,h} \tag{24}$$

E. PV Unit Constraint

The PV units are used for generating electricity from available solar energy resources. According [32], in 2019, North Carolina developed 5.81% of its electricity through solar power and ranked second in total installed photovoltaics in the U.S. Thus, PV modules would be an appropriate candidate for consideration in this study compared with other types of renewables [33]–[35]. Constraint (25) calculates the output power of the PV farm according to available solar irradiance.

$$P^{PV}_{s,t,k,i} = P^{STC}_{k,i} + G^{INC}_{s,t,k,i} / G^{STC} [1 - k\,(T_c - T_r)]/1000 \tag{25}$$

F. Power Flow Constraints

AC power flow equations are modeled as (26)–(30). The proposed formulation also incorporated MERs' required capacities and locations, which will used for delivering power by MERs accordingly.

Constraints (26)–(27) show each network bus's active and reactive power balance, considering DGs, ESSs, PV units, MERs, EVs and loads. Constraint (29) limits the active power flow of distribution lines into upper and lower boundaries, and (30) additionally indicates the allowable range of bus voltage magnitudes.

$$\begin{aligned} &\sum_{g} M^{DGB}_{b,k,g} \times P^{DG}_{s,t,g,k} + \sum_{e} M^{ESSB}_{b,k,e} \\ &\quad \times \left(P^{ESS,Dch}_{s,t,k,e} - P^{ESS,Ch}_{s,t,k,e}\right) \\ &\quad + \sum_{i} M^{PVB}_{b,k,i} \times P^{PV}_{s,t,k,i} + \sum_{m} M^{MERB}_{b,k,m} \times P^{MER}_{s,t,k,m} \\ &\quad + \sum_{j} M^{EVB}_{b,k,j} \times P^{TEV}_{s,t,k,j} \\ &= \sum_{d} M^{DB}_{b,k,d} \times P^{Demand}_{s,t,k,d} + \sum_{L} M^{LB}_{b,k,L} \times P^{L}_{s,t,k,m} \\ &\quad + \sum_{d} M^{LB}_{b,k,d} \times P^{shed}_{s,t,k,d} \end{aligned} \tag{26}$$

$$\begin{aligned} &\sum_{g} M^{DGB}_{b,k,g} \times Q^{DG}_{s,t,g,k} + \sum_{e} M^{ESSB}_{b,k,e} \\ &\quad \times \left(Q^{ESS,Dch}_{s,t,k,e} - Q^{ESS,Ch}_{s,t,k,e}\right) \\ &\quad + \sum_{i} M^{PVB}_{b,k,i} \times Q^{PV}_{s,t,k,i} + \sum_{m} M^{MERB}_{b,k,m} \times Q^{MER}_{s,t,k,m} \\ &\quad + \sum_{j} M^{EVB}_{b,k,j} \times Q^{TEV}_{s,t,k,j} \\ &= \sum_{d} M^{DB}_{b,k,d} \times Q^{Demand}_{s,t,k,d} + \sum_{L} M^{LB}_{b,k,L} \times Q^{L}_{s,t,k,m} \\ &\quad + \sum_{d} M^{LB}_{b,k,d} \times Q^{shed}_{s,t,k,d} \end{aligned} \tag{27}$$

$$Q^{c}_{s,t,k,k} \le \overline{Q^{c}_{k,b}} \tag{28}$$

$$-\overline{P^{L}_{k,L}} \le P^{L}_{k,L} \le \underline{P^{L}_{k,L}} \tag{29}$$

$$\overline{V} \le V_{s,t,k,b} \le \underline{V} \tag{30}$$

$$\begin{cases} P^{shed}_{s,t,d,k} \le P^{Demand}_{s,t,d,k} \\ Q^{shed}_{s,t,d,k} \le Q^{Demand}_{s,t,d,k} \end{cases} \tag{31}$$

A distribution locational marginal price (DLMP) methodology has been used to linearize the load flow formulation in distribution networks [36]. The proposed method applies an appropriate linear approximation to compute both the magnitude and angle of bus voltages. The reactive power flows of the lines are considered in the proposed method. Constraints (32)–(35) represent linearized power flow equations.

$$\begin{aligned} P^{L}_{s,t,k,l} &= Z^{LP}_{s,t,k,l} + F^{A}_{k,L} \times \sum_{b} \left(\delta_{s,t,k,b} - \delta_{s,t,k,b'}\right) \\ &\quad + F^{B}_{k,L} \times \sum_{b} \left(V_{s,t,k,b} - V_{s,t,k,b'}\right) \end{aligned} \tag{32}$$

$$\begin{aligned} Q^{L}_{s,t,k,l} &= Z^{LQ}_{s,t,k,l} + F^{B}_{k,L} \times \sum_{b} \left(\delta_{s,t,k,b} - \delta_{s,t,k,b'}\right) \\ &\quad + F^{A}_{k,L} \times \sum_{b} \left(V_{s,t,k,b} - V_{s,t,k,b'}\right) \end{aligned} \tag{33}$$

$$F^{A}_{k,L} = r_{k,L} \big/ \left(r^2_{k,L} + x^2_{k,L}\right) \tag{34}$$

$$F^{B}_{k,L} = x_{k,L} \big/ \left(r^2_{k,L} + x^2_{k,L}\right) \tag{35}$$

G. Objective Function

The aim would be to achieve maximum resilience of the system after the occurrence of the hurricane by using either reconfiguration or MG resources such as MERs, ESSs, and EVs. The proposed resilience objective function is shown in (36). In this equation, the resilience index (R) is improved by maximizing system performance $F(t)$ or minimizing operation cost G. According to (37), $F(t)$ can be determined by the total electrical energy supplied to consumers based on their weighting priority. The formulation is updated in (38) by selecting T^{CL} as the service time of the load restoration after the hurricane. It is worth noting that the variable T^{CL} is determined based on either Dijkstra's algorithm or reconfiguration in the integrated framework. Considering the T^{CL}, a well-known mixed-integer non-linear programming (MINLP) was utilized then converted to a linear problem to solve the problem accurately. Equations (39)-(40) indicate the operation cost of the CCMG, which makes it possible to restore the system with the minimum cost.

$$R = \gamma \times \int_{t_r}^{t_r+T^0} F(t)dt - G \tag{36}$$

$$F(t) = \sum_k \sum_m W_{m,k} P^D_{m,k,t}, t \in \left[t_r, t_r + T^0\right] \tag{37}$$

$$\begin{aligned} R &= \int_{t_r}^{t_r+T^0} \left(\sum_{\forall m \in \Omega^B} W_{m,k,t} P^D_{m,k,t} \right) dt - G \\ &= \sum_{\forall m \in \Omega^B} W_{m,k} \int_{t_r}^{t_r+T^0} P^D_{m,k,t} dt - G \\ &= \sum_{\forall m \in \Omega^B} W_{m,k} \int_{t_r}^{t_r+T^{CL}} P^D_{m,k,t} dt - G \\ &= \sum_{\forall m \in \Omega^B} W_{m,k} P^D_{m,k} T^{CL}_{m,k} - G \end{aligned} \tag{38}$$

$$\begin{aligned} G = {} & \beta_1 \sum_k P^{DG}_{s,t,g,k} \times \pi^{DG}_{g,k} + \beta_2 \sum_m P^{MER}_{s,t,m,k} \times \pi^{MER}_{m,k} \\ & + \beta_3 \sum_e \pi^{ESS}_{k,e} \times \left(P^{ESS,Ch}_{s,t,k,e} + P^{ESS,Dch}_{s,t,k,e} \right) \\ & + \beta_4 \sum_j P^{EV}_{s,t,k,j} \times \pi^{TEV}_{k,j} \\ & + \beta_5 \sum_d P^{DR}_{s,t,k,d} \times \pi^{DR}_{k,d} + \beta_6 \sum_d P^{shed}_{s,t,k,d} \times VOLL \end{aligned} \tag{39}$$

$$\sum_{i=1}^{6} \beta_i = 1 \tag{40}$$

The diagram of the proposed approach is depicted in Fig. 2. Initially, all the objective functions and data related to resources initialize, specifically the MERs's location and capacities. Then, the control approache is implemented by evaluating the objective functions and reporting the system measurement as a metrics reference. Next, MERs short-path algorithm determines the optimum path for supplying power to the loads. Reconfiguring the network is performed based on the rerouting MERs and available resources as well. In the case of not fulfilling the system performance criterion requirements, the rerouting algorithm continues until it attains the optimum solution for the reconfiguration. Finally, a metrics assessment evaluates the control system performance.

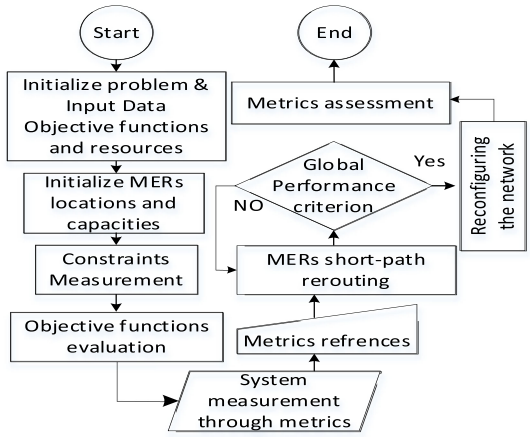

Fig. 2. The proposed integrated control and management system for CCMGs relies upon the metrics assessment.

III. Short-Path Routing Algorithm

As a well-known methodology, Dijkstra's algorithm is used for finding optimum routes to deliver MERs to either islanded buses or buses with a shortage of power. One of the merits of Dijkstra's algorithm is that it can find optimum solutions to the one-to-all shortest path problem. The optimum path is determined from a candidate node *s* to all the other nodes of the weighted network. MER benefit from big satellite data before the occurrence of the hurricane, which would help them move to the most appropriate locations close enough to the hurricane route for rapid power delivery to the damaged buses.

In the proposed integrated optimization framework, the optimum routes are calculated for all the nodes. When the number of damaged buses overtakes the available truck-mounted MERs, the priority goes to the buses with the shortest path. Furthermore, obstructed routes (edges) are omitted from Dijkstra's algorithm. To model the physical distance between two different nodes, the weight C_{ij} for edge (i,j) is used in this study. More details on the steps taken and implementation of the algorithm can be found in [23].

IV. Numerical Simulations

The structure of the proposed two-phase evaluation framework through specific metrics is depicted in Fig. 3. In this structure, the resiliency function is maximized by optimizing the exchange among CCMGs associated with DGs, PVs, EVs, MERs, and reconfiguration, and provides a road map for MERs. Then, the control system is evaluated by specific metrics to assess the control system performance. An appropriate control and optimization approach for the interdependency of the power

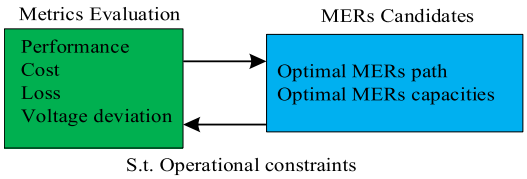

Fig. 3. Proposed integrated resiliency metrics evaluation for CCMGs.

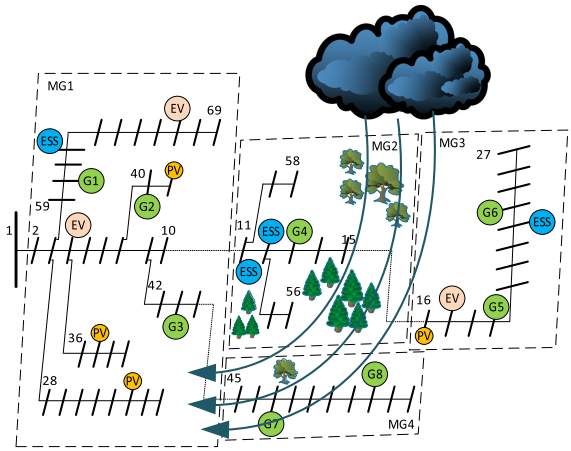

Fig. 4. Schematic of the CCMG considering the hurricane.

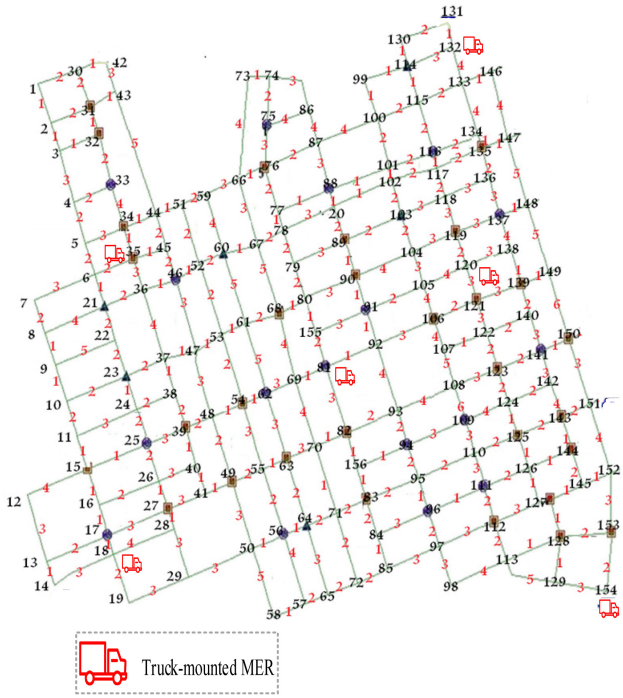

Fig. 5. Transportation road map and network topology (a unit = 2.6 miles).

TABLE II
ELECTRICITY PRICES UTILIZED IN THE TEST SYSTEM

Parameter	Value [$/kWh]
$\pi_{g,k}^{DG}$	0.1
$\pi_{m,k}^{MER}$	0.7
$\pi_{k,e}^{ESS}$	0.65
$\pi_{k,j}^{TEV}$	0.6
$\pi_{k,d}^{DR}$	0.5

TABLE III
PROPOSED CASE STUDIES BASED ON THE UTILIZED COMPONENTS AND LOAD LEVEL

Case No.	ESS	MER	PV	EV	Load level
1	0	0	0	0	1
2	1	0	0	0	1
3	0	1	0	0	1
4	0	0	1	0	1
5	0	0	0	1	1
6	1	1	1	1	1
7	1	1	1	1	1.05
8	1	1	1	1	0.95

supply by MERs is vital for the islanded load. In other words, first, the shortest path of MERs is required as a function of vegetation limitations (damage, availability, length). Then, the best candidate locations and MERs with reasonable capacity must be identified to supply the islanded load. Thereafter, the resiliency index is maximized based on the evaluation of the metrics (reconfiguration, connected MGs) to improve the general objectives.

The single-line diagram of the CCMG test system consists of four interconnected MGs with the hurricane incident across the middle of the network as shown in Fig. 4 [5]. There are four tie switches located between buses 27–65, 50–59, 15–46, 13–21, and 11–43, and a total of 68 sectionalizing switches. The technical characteristics of the DGs in each MG and the damaged power lines and roads are taken from [23]. According to the geographic data illustrated in Fig. 5, there are overall 154 nodes (black number) with route distances (red number) and 269 edges [24], [37]–[39].

The six truck-mounted MERs in the network are appropriately placed in their locations before the occurrence of the hurricane. The locations of MERs, as shown in Fig. 5, are visible in the network topology. In this study, the length of the outage time (T^0) is anticipated based on the distribution system, crew experiences and available prediction methods after the hurricane, which is considered 5 hours on average in this study.

In this study, the maximum and minimum SOC of ESS and EV is considered 100% and 10%, respectively. Charging and discharging efficiencies of EV and ESS is assumed 95%. Battery capacity and *VOLL* are considered 24 kWh and US$1000, respectively. Electricity price data is also provided in Table II. According to Table III, eight case studies are introduced to illustrate the merits of the proposed resilient framework. Case studies are presented based on different system configurations that rely on the availability of electrical resources (1 stands for available and 0 for unavailable). Case 6 demonstrates the proposed framework of this paper benefiting from all types of resources. Cases 7 and 8 also study the effects of load levels on the optimization results. The focus is to explore the RESs role and the ESS/MERs separately and jointly to evaluate the control system performance within the metrics analysis. As shown in Table III, the case scenarios are defined based on the role of the individual and cooperation of the resources such as RES,

TABLE IV
COMPARATIVE RESULTS BASED ON THE OF DIFFERENT CASE STUDIES

Case No.	Cost (US$)	ENS (kWh)	Interrupted Loads
1	3,300,347	34,679.5	11,12,17,18,34,35,37,39,52,59,61,62,66,67,68
2	3,200,349	32,068.5	11,12,17,18,34,35,37,39,52,59,61,62,66,67,68
3	2,837,626	22,277.6	11,12,17,18,34,35,37,39,52,61,62,66,67,68
4	3,273,440	30,576.2	11,12,17,18,34,35,39,52,59,61,62,66,67,68
5	3,030,523	28,972.8	11,12,34,35,37,39,52,59,61,62,66,67
6	2,318,272	10,885.9	11,34,35,39,52,61,62,66,67
7	2,467,276	12,116.6	11,34,35,39,52,61,62,66,67,68
8	2,169,381	11,318.2	11,34,35,39,52,61,62,66,67

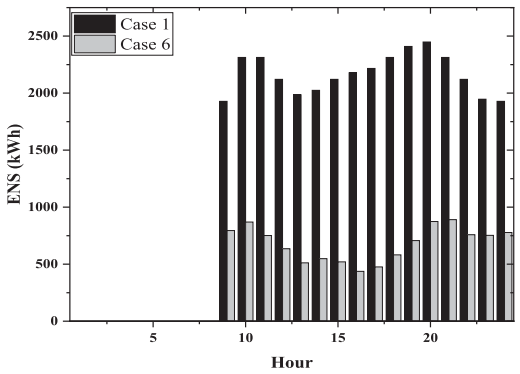

Fig. 6. Comparative results of the ENS values for the base case (case 1) and the proposed case (case 6).

ESS, MERs, etc., to explore the efficacy of these resources with respect to each other in the context of metrics assessment.

The comparative results of power generation cost, ENS, and interrupted loads are indicated in Table IV. In Case 3, power generation cost and ENS value are notably reduced to US$2837626 and 22277.6 kWh, respectively. It shows the effectiveness of track-mounted MREs in post-hurricane load restorations. However, the proposed framework of this study in case 6 has resulted in the minimum power generation cost and ENS value. For instance, the loads on busses 12 and 59 are notably restored in the sixth case. Utilization of EVs also has a more significant on reducing ENS and power generation costs than PV units and ESSs.

In this study, the effects of different values of load levels on the optimization results are analyzed in cases 7 and 8. Based on the results, slight growth in load level (1.05) will increase power generation cost and the amounts of ENS; however, the value is not significant in the proposed framework, in which all the mentioned components are utilized. Conversely, a small reduction in load level (0.95) decreases power generation cost but increases the ENS value. It also does not change the number of interrupted loads compared to the fixed load level in case 6. In addition, a comparison has been made between the values in case 1 and case 6. As can be seen from Fig. 6, the utilization of the electrical components has reduced the ENS values over the day. The base case (Case 1) does not benefit from any of the proposed electrical components. As a result, the ENS values in the base case are significant at various hours of the day.

Table V shows the optimum path of MERs from simulations. MERs start from the predetermined locations and pass the nodes indicated in Table V to arrive at the islanded buses. More details on the performance of the MERs are given in Table VI. The maximum power of all MERs has been considered as 230 kW. Table VII shows the post-hurricane operation of MERs at different hours of the day. As illustrated, red color indicates the driving mode of MREs, and green color shows the connected mode of MERs. According to the results, MER 1 connects to the target bus earlier than other MERs and provides electricity until the capacity limitation is reached. However, MER 5 spends most of the hours to traveling to the targeted bus and supplies only two hours after connecting. Generally, increasing MERs' travel time will increase the total ENS and decrease the network's resilience.

TABLE V
OPTIMAL ROUTE-FINDING RESULTS FOR EACH MER

MER No.	Optimal Routes									
1	20	89								
2	35	6	21	8						
3	81	92	91	90	89					
4	120	119	104							
5	132	114	99	100	101	88	20	89		
6	154	153	128	127	126	125	124	123	141	

TABLE VI
PERFORMANCE OF TRUCK-MOUNTED MERS IN POST-HURRICANE PERIOD

MER No.	Start	End	Duration	SOC_0	P_{max}	H_{full}	H_{left}
1	20	89	2	2200	230	9	0.56
2	35	8	7	2400	230	10	0.4
3	81	89	4	2350	230	10	0.2
4	120	104	5	2250	230	9	0.8
5	132	89	11	2300	230	10	0
6	154	141	12	2000	230	8	0.6

The maximum net power supply occurs at 23:00, when all the MREs are in connecting mode. It should be noted that even if a MER is connected to the targeted bus earlier than other available MERs, it does not mean that the desired MER can maintain power to the loads until the end of the day. They should be fully charged before the hurricane to support damaged grid structures as much as possible for during and post contingency situations. Therefore, in the proposed optimization model only the discharge mode of MERs is considered, and, as a result, discharge efficiency is considered in the calculation of SOC of the MERs.

In detail, MRE 1 connects to the target bus at 11:00 and supplies the loads until 20:00. On the other side, MER 3 connects to the target load at 13:00 while providing electricity to the day's end. The total power supplied by MER 1 and MER 2 are 2198.8 kWh and 2392 kWh, respectively. This shows that MER 3 was able to provide more electricity than MER 1 during the day. Therefore, it is concluded that the MERs' power capacity also plays a crucial role in electrifying the loads.

The actual time horizon for the control and management system to update the control actuator is approximately two minutes, which is a reasonable time for the tertiary control layer considering typical decision-making is each hour. In addition, it makes the proposed approach an excellent candidate for real-time instantiation assessed via controller hardware-in-the-loop (CHIL). It is worth noting, that the availability of the DGs, for instance, MERs may impose some delay to the control system update. In other words, MERs with a travel distance of two hours or more will not be considered as the potential solutions for islanded loads given that MERs with travel times less than 1

TABLE VII
HOURLY SUPPLIED POWER BY TRUCK-MOUNTED MERS IN POST-HURRICANE

Operation Mode	Driving		Connected													
Hours	9	10	11	12	13	14	15	16	17	18	19	20	21	22	23	24
MER1	0	0	1	1	1	1	1	1	1	1	1	1	1	1	1	1
MER2	0	0	0	0	0	0	0	1	1	1	1	1	1	1	1	1
MER3	0	0	0	0	1	1	1	1	1	1	1	1	1	1	1	1
MER4	0	0	0	0	0	1	1	1	1	1	1	1	1	1	1	1
MER5	0	0	0	0	0	0	0	0	0	0	0	0	1	1	1	1
MER6	0	0	0	0	0	0	0	0	0	0	0	0	0	0	1	1
Supplied Power (kWh)	0	0	230	230	230	230	230	230	230	230	230	128.8	0	0	0	0
	0	0	0	0	0	0	0	230	230	230	230	230	230	230	230	230
	0	0	0	0	230	230	230	230	230	230	230	230	230	230	230	92
	0	0	0	0	0	230	230	230	230	230	230	230	230	230	230	46
	0	0	0	0	0	0	0	0	0	0	0	0	230	230	230	230
	0	0	0	0	0	0	0	0	0	0	0	0	0	0	230	230
Net Power (kWh)	0	0	230	230	460	690	690	920	920	920	920	818.8	920	920	1150	828

hour are more desirable for rapid restoration and reconfiguration considerations.

Moreover, the MER 6 has traveled more distance than other MREs (12 hours). On the other hand, MER 1 has the least travel distance with 2 hours of duration.

V. METRICS EVALUATION OF THE CONTROL SYSTEM

Control and management systems integrate a variety of objective functions that depend upon the application. The metrics evaluation of system-level objective functions during optimization improves the control system performance in the context of connected MGs for resiliency; specifically, such performance metrics as: voltage deviation, line loss, and number of restored loads [40]. Thus, the objective functions such as the cost, performance, voltage, number of restored loads and power loss can be evaluated to assess the proposed control system. At this stage, a holistic metrics evaluation of the control and management system is implemented for the system under test in emergency post-disaster operations.

A. Voltage Deviation

By considering the voltage drops and surge avoided in the system, deviation of voltage formulates as:

$$\min J\ \left(V(t)\right) = \sum_{t=1}^{N_T} \left\{ \sum_{bb=1}^{N_{bb}} \left|1 - V_{bb}^{t}\right| \right\} \tag{41}$$

The bus voltage must be kept in the limit, 0–6% approximately to minimize (41).

B. Line Loss

The power-sharing set points of the energy resources can fluctuate due to line loss. The net line loss will increase or decrease at each management interval depending upon the load profile. The line losses are calculated via (42).

$$\min J\ \left(P_l\left(t\right)\right) = \sum_{t=1}^{N_T} \left\{ \sum_{l=1}^{N_l} \frac{V_l^{t\,2}}{Z_l} \cos\theta_l \right\} \tag{42}$$

TABLE VIII
METRICS EVALUATION OF THE PROPOSED CONTROL SYSTEM FOR RESILIENT CCMGS

Case No	Performance	Performance Improvement (%)	Number of revived loads	Voltage Deviation (P.U)	Line loss (kWh)
1	0.6393	-	-	6.8705	6442.5
2	0.6476	1.30	56	6.7732	6097.5
3	0.7403	15.78	600	6.2839	5746.6
4	0.6537	2.25	62	6.8088	5916.1
5	0.6925	8.31	242	6.3540	6311.9
6	0.8463	32.37	1562	5.7988	4744.5
7	0.8398	-	-	5.8098	5066.6
8	0.8503	-	-	5.7502	5079.6

C. Performance

The financial burden associated with DGs and RES turn-ON/OFF status, maintenance, infrastructural charges, utility fees or government dues (tax), and energy transaction from MG to the grid, composes the performance objective functions as defined as CAPEX and OPEX. The performance metric is formulated as (43).

$$\max J\left(F\left(X\right)\right) = F\left(t\right) = \sum_{k}\sum_{m} W_{m,k} P_{m,k,t}^{D},\ t \in \left[t_r, t_r + T^0\right] \tag{43}$$

D. Number of Restored Loads

The number of customers who are back to normal operation mode via supply through DRs and MERs safely is considered an important metric for the control and management system performance evaluation.

The metrics evaluation results of the proposed system are summarized in Table VIII.

As it can be seen, the maximum performance improvement of the management system belongs to the third and sixth case studies with over 15% and 32%, respectively. Also, the results show the superiority of MERs as DRs over the other options for increasing the resiliency index of the distribution system. The performance of the proposed control and management system is improved less than 3% by using either solid ESSs in locations or PVs, which is reasonable because of weather-related limitations on the occasions. The lowest line loss (4744.5 kWh) is dedicated

to the sixth case study when all DERs (MERs, PV, EVs, and ESSs) are contributed for supplying the power to the loads within minimum time and shortest path. The second and third lowest line losses are determined by the third and fourth case studies when using the MERs and EVs, respectively. Also, the number of restored loads in the sixth case (1562) is higher than the others to increase the resiliency of the islanded buses. The second-highest number of restored loads is dedicated to the third case with MERs benefits.

VI. Conclusion

A metrics analysis framework is investigated to assess the control and management system ability for attaining the highest resiliency index of the CCMGs in the post-hurricane period. In the proposed approach, several resources such as truck-mounted MERs, EVs, ESSs, and DR program are utilized to increase the systems' flexibility over traditional distribution systems. Truck-mounted MERs as a potential candidate are used to supply the islanded or damaged buses after the hurricane in the outage area that is due to vegetation issues. To this end, Dijkstra's algorithm is applied to find optimal routes for MERs' distance of travel. To evaluate the proposed method performance, eight case studies are introduced based on utilized components and load levels. Simulation results revealed that the proposed framework of this study led to the minimum power generation cost and total ENS value as 2318272 US$ and 10885.9 kWh, respectively as well as the metrics evaluation analysis with 32.37% performance improvement. The main goal of this study is to define an appropriate assessment framework applicable for real-time applications for control hardware-in-the-loop (CHIL) for large-scale networks in the future.

Acknowledgment

The authors would like to thanks Mr. Payam Ramezani Badr for his valuable contribution on this study.

References

[1] B. Papari *et al.*, "Distributed control in hybrid AC-DC microgrids based on a hybrid MCSA-ADMM algorithm," *IEEE Open J. Ind. Appl.*, vol. 2, pp. 121–130, Apr. 2021.

[2] G. Ozkan, P. H. Hoang, P. R. Badr, C. S. Edrington, and B. Papari, "Real-time thermal management for two-level active rectifier with finite control set model predictive control," *Int. J. Elect. Power Energy Syst.*, vol. 131, 2021, Art. no. 107057.

[3] B. Papari, C. S. Edrington, G. Ozkan, and P. R. Bader, "Stochastic analysis of regenerative braking energy of urban transportation system associated with Plug-in electrical vehicle in smart city," in *Proc. IEEE 4th Int. Conf. DC Microgrids*, Arlington, VA, USA, 2021, pp. 1–5.

[4] S. L. Cutter, "The changing nature of hazard and disaster risk in the anthropocene," *Ann. Amer. Assoc. Geographers*, pp. 1–9, 2020.

[5] C. G. Rieger, "Notional examples and benchmark aspects of a resilient control system," in *Proc. 3rd Int. Symp. Resilient Control Syst.*, 2010, pp. 64–71.

[6] H. Mehrjerdi, "Resilience-robustness improvement by adaptable operating pattern for electric vehicles in complementary solar-vehicle management," *J. Energy Storage*, vol. 37, 2021, Art. no. 102454.

[7] D. Henry and J. E. Ramirez-Marquez, "Generic metrics and quantitative approaches for system resilience as a function of time," *Rel. Eng. Syst. Saf.*, vol. 99, pp. 114–122, 2012.

[8] D. A. Reed, K. C. Kapur, and R. D. Christie, "Methodology for assessing the resilience of networked infrastructure," *IEEE Syst. J.*, vol. 3, no. 2, pp. 174–180, Jun. 2009.

[9] S. Bahramirad, A. Khodaei, J. Svachula, and J. R Aguero, "Building resilient integrated grids: One neighborhood at a time," *IEEE Electrific. Mag.*, vol. 3, no. 1, pp. 48–55, Mar. 2015.

[10] Y. Wang, C. Chen, J. Wang, and R. Baldick, "Research on resilience of power systems under natural Disasters—A review," *IEEE Trans. Power Syst.*, vol. 31, no. 2, pp. 1604–1613, Mar. 2016.

[11] G. Dong and Z. Chen, "Data-driven energy management in a home microgrid based on Bayesian optimal algorithm," *IEEE Trans. Ind. Inform.*, vol. 15, no. 2, pp. 869–877, Feb. 2019.

[12] S. Mohagheghi and F. Yang, "Applications of microgrids in distribution system service restoration," in *Proc. ISGT*, 2011, pp. 1–7.

[13] M. He and M. Giesselmann, "Reliability-constrained self-organization and energy management towards a resilient microgrid cluster," in *Proc. IEEE Power Energy Soc. Innov. Smart Grid Technol. Conf.*, Washington, DC, USA, 2015, pp. 1–5.

[14] C. Chen, J. Wang, F. Qiu, and D. Zhao, "Resilient distribution system by microgrids formation after natural disasters," *IEEE Trans. Smart Grid*, vol. 7, no. 2, pp. 958–966, Mar. 2016.

[15] K. Dehghanpour, C. Colson, and H. Nehrir, "A survey on smart agent-based microgrids for resilient/self-healing grids," *Energies*, vol. 10, no. 5, 2017, Art. no. 620.

[16] Z. Wang and J. Wang, "Self-healing resilient distribution systems based on sectionalization into microgrids," *IEEE Trans. Power Syst.*, vol. 30, no. 6, pp. 3139–3149, Nov. 2015.

[17] F. Yang, X. Feng, and Z. Li, "Advanced microgrid energy management system for future sustainable and resilient power grid," *IEEE Trans. Ind. Appl.*, vol. 55, no. 6, pp. 7251–7260, Nov./Dec. 2019.

[18] A. Alsubaie *et al.*, "A platform for disaster response planning with inter-dependency simulation functionality," in *Proc. Int. Conf. Crit. Infrastruct. Protection*, Berlin, Heidelberg, Germany, 2013, pp. 183–197.

[19] G. Huang, J. Wang, C. Chen, J. Qi, and C. Guo, "Integration of preventive and emergency responses for power grid resilience enhancement," *IEEE Trans. Power Syst.*, vol. 32, no. 6, pp. 4451–4463, Nov. 2017.

[20] M. Panteli, D. N. Trakas, P. Mancarella, and N. D. Hatziargyriou, "Power systems resilience assessment: Hardening and smart operational enhancement strategies," *Proc. IEEE*, vol. 105, no. 7, pp. 1202–1213, Jul. 2017.

[21] B. Chen, C. Chen, J. Wang, and K. L. Butler-Purry, "Sequential service restoration for unbalanced distribution systems and microgrids," *IEEE Trans. Power Syst.*, vol. 33, no. 2, pp. 1507–1520, Mar. 2018.

[22] Z. Bie, Y. Lin, G. Li, and F. Li, "Battling the extreme: A study on the power system resilience," *Proc. IEEE*, vol. 105, no. 7, pp. 1253–1266, Jul. 2017.

[23] S. A. Arefifar, M. Ordonez, and Y. A. R. I. Mohamed, "Energy management in multi-microgrid systems—Development and assessment," *IEEE Trans. Power Syst.*, vol. 32, no. 2, pp. 910–922, Mar. 2017.

[24] A. Kavousi-Fard, M. Wang, and W. Su, "Stochastic resilient post-hurricane power system recovery based on mobile emergency resources and reconfigurable networked microgrids," *IEEE Access*, vol. 6, pp. 72311–72326, 2018.

[25] S. Lei, J. Wang, C. Chen, and Y. Hou, "Mobile emergency generator pre-positioning and real-time allocation for resilient response to natural disasters," *IEEE Trans. Smart Grid*, vol. 9, no. 3, pp. 2030–2041, May 2018.

[26] Z. Yang, P. Dehghanian, and M. Nazemi, "Seismic-resilient electric power distribution systems: Harnessing the mobility of power sources," *IEEE Trans. Ind. Appl.*, vol. 56, no. 3, pp. 2304–2313, May/Jun. 2020.

[27] Z. Li, M. Shahidehpour, F. Aminifar, A. Alabdulwahab, and Y. Al-Turki, "Networked microgrids for enhancing the power system resilience," *Proc. IEEE*, vol. 105, no. 7, pp. 1289–1310, Jul. 2017.

[28] Q. Zhou, M. Shahidehpour, A. Paaso, S. Bahramirad, A. Alabdulwahab, and A. Abusorrah, "Distributed control and communication strategies in networked microgrids," *IEEE Commun. Surv. Tut.*, vol. 22, no. 4, pp. 2586–2633, Oct./Dec. 2020.

[29] J. Wang and X. Lu, "Sustainable and resilient distribution systems with networked microgrids," *Proc. IEEE*, vol. 108, no. 2, pp. 238–241, Feb. 2020.

[30] R. Bahmani, H. Karimi, and S. Jadid, "Stochastic electricity market model in networked microgrids considering demand response programs and renewable energy sources," *Int. J. Elect. Power Energy Syst.*, vol. 117, 2020, Art. no. 105606.

[31] H. Mirzaei, Z. Li, and Y. Parvini, "Validation and sensitivity analysis of a fractional order model of a Lithium ion battery via impedance spectra and temporal duty cycles," in *Proc. Amer. Control Conf.*, 2020, pp. 359–364.

[32] SEIA, Comms Team, "Solar Market Insight Report 2019 Q3," Accessed: Sep. 17, 2019. [Online]. Available: https://www.seia.org/
[33] N. L. Dehghani, A. B. Jeddi, and A. Shafieezadeh, "Intelligent hurricane resilience enhancement of power distribution systems via deep reinforcement learning," *Appl. Energy*, vol. 285, 2021, Art. no. 116355.
[34] U.S. Department of Energy, "DOE responds as hurricane harvey impacts texas," Accessed: Aug. 25, 2017. [Online]. Available: https://www.energy.gov/oe/articles/doe-responds-hurricane-harvey-impacts-texas
[35] U.S. Department of Energy, Office of Energy Efficiency & Renewable Energy, "Weathering the storm: Supporting states and U.S. territories during hurricane season," Accessed: May 26, 2021. [Online]. Available: https://www.energy.gov/eere/articles/weathering-storm-supporting-states-and-us-territories-during-hurricane-season
[36] R. Nourollahi, P. Salyani, K. Zare, and B. Mohammadi-Ivatloo, "Resiliency-oriented optimal scheduling of microgrids in the presence of demand response programs using a hybrid stochastic-robust optimization approach," *Int. J. Elect. Power Energy Syst.*, vol. 128, 2021, Art. no. 106723.
[37] S. H. Huang and P. C. Lin, "Vehicle routing–scheduling for municipal waste collection system under the "Keep Trash off the Ground Policy," *Omega*, vol. 55, pp. 24–37, 2015.
[38] M. Ansari, M. Zadsar, H. Zareipour, and M. Kazemi, "Resilient operation planning of integrated electrical and natural gas systems in the presence of natural gas storages," *Int. J. Elect. Power Energy Syst.*, vol. 130, 2021, Art. no. 106936.
[39] M. Ansari, M. Zadsar, S. S. Sebtahmadi, and M. Ansari, "Optimal sizing of supporting facilities for a wind farm considering natural gas and electricity networks and markets constraints," *Int. J. Elect. Power Energy Syst.*, vol. 118, 2020, Art. no. 105816.
[40] P. Ramezani, C. S. Edrington, P. H. Hoang, N. Deb, B. Papari, and G. Ozkan, "MetaMetric approach in performance assessment of system level controllers for different operational objectives," in *Proc. IEEE Texas Power Energy Conf.*, College Station, TX, USA, 2020, pp. 1–6.

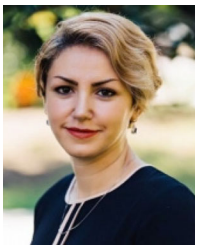

Behnaz Papari (Member, IEEE) received the B.S. and M.Sc. degrees in electrical engineering in 2008 and 2011, respectively, and the Ph.D. degree in electrical and electronics engineering from Florida State University, Tallahassee, FL, USA, in 2018. She is currently an Assistant Professor with Marine Engineering Technology at Texas A&M. She has expertise in power systems controls with an emphasis on modeling, analysis, planning, and optimization. She was an Assistant Professor of practice with Energy Production and Infrastructure Center (EPIC), UNC Charlotte. She joined the Texas A&M, where she became known for her research in the areas of distributed controls and secure control framework under uncertainty, cyber-physical security, control of stand-alone ship power system and utility-interactive energy systems, applications on energy system modeling, and stochastic optimization, AI-based distributed control of smart grids, and real-time power distribution system simulation and hardware-in-the-loop instantiation.

Christopher S. Edrington (Senior Member, IEEE) received the B.S. degree in engineering from Arkansas State University, Jonesboro, AR, USA, in 1999, and the M.S. and Ph.D. degrees in electrical engineering from Missouri Science and Technology, Rolla, MO, USA, in 2001 and 2004, respectively. He was a GAANN and IGERT Fellow with Missouri Science and Technology. From 2004 to 2007, he was an Assistant Professor of electrical engineering with the College of Engineering, Arkansas State University. From 2007 to 2019, he held the ranks of a Assistant, Associate, and Full Professor of electrical and computer engineering with the FAMU-FSU College of Engineering and was the lead for the Energy Conversion and Integration thrust for the Florida State University-Center for Advanced Power Systems. In 2019, he joined Clemson University, Clemson, SC, USA, as the Warren H. Owen Distinguished Professor of electrical and computer engineering where he leads RT-COOL (Real-Time COntrol and Optimization Laboratory). His research interests include modeling, simulation, optimization and control of electromechanical drive systems, applied power electronics, integration of renewable energy, storage, and pulse power loads, and HIL (hardware in the loop) VV&A experimentation.

Mojtaba Ghadamyari (Member, IEEE) studied the electrical engineering from Shahid Beheshti University, Tehran, Iran. He is currently researching on power system. He has authored or coauthored more than five journal papers in the fields of reliability, distributed generation, energy and renewable resource. His current research interests include reliability, distributed generation, microgrid, and renewable energy.

Mostafa Ansari (Member, IEEE) received the B.S. degree in electrical engineering from Shahid Beheshti University, Tehran, Iran, in 2014, and the M.S. degree in electrical engineering from the Isfahan University of Technology, Isfahan, Iran, in 2017. From 2017 to 2019, he was with the Isfahan University of Technology, Niroo Research Institute, and Monenco Iran Consulting Engineering Company as a Researcher. Since 2019, he has been a Senior Electrical Engineer with the R&D and Investment Department of Tamin Energy Development Company, SHASTA, Iran. His current research interests include power systems and electricity markets modeling and analysis, optimization in multienergy systems and sustainable integration of renewable energy sources into electricity grids.

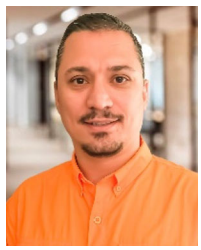

Gokhan Ozkan (Member, IEEE) received the B.Sc. degree from Electric Education Department, Marmara University, Istanbul, Turkey, in 2006, the B.Sc. (as a valedictorian) and M.Sc. degrees from Energy System Engineering Department, Erciyes University, Kayseri, Turkey, in 2014 and 2016, respectively, and the Ph.D. degree from Electrical and Computer Engineering Department, Florida State University, Tallahassee, FL, USA, in 2019. In 2020, he joined Clemson University, Clemson, SC, USA, as a Postdoctoral Fellow. Since 2021, he has been a Research Assistant Professor with the Holcombe Department of Electrical and Computer Engineering. He is also a Manager of Real-Time COntrol and Optimization Laboratory (RT-COOL). His main research interests include model predictive control in power converters and drives, active thermal management and fault-tolerant control, distributed controls, power and energy management, and real-time power.

Badrul Chowdhury (Senior Member, IEEE) received the Ph.D. degree in electrical engineering from the Virginia Tech, Blacksburg, VA, USA, in 1987. He is currently a Professor with the Department of Electrical and Computer Engineering with joint appointment with the Department of Systems Engineering and Engineering Management, University of North Carolina at Charlotte, Charlotte, NC, USA. His current research interests include power system modeling, analysis and control, renewable and distributed energy resource modeling and integration in smart grids, and resilient community microgrids. He is the Editor-in-Chief of the IEEE TRANSACTIONS ON SUSTAINABLE ENERGY.